Theor Chim Acta (1995) 92: 369–381

Theoretica Chimica Acta

A geometry optimization benchmark using highly correlated wavefunctions (FCI and MRD-CI)

Josep Maria Anglada[1], **Josep Maria Bofill**[2]

[1] C.I.D.-C.S.I.C., Jordi Girona Salgado 18-26, E-08034 Barcelona, Catalunya, Spain
[2] Departament de Química Orgànica, Universitat de Barcelona, Martí i Franquès, 1, E-08028 Barcelona, Catalunya, Spain

Received January 18, 1995/Accepted June 12, 1995

Summary. Full configuration interaction (FCI) geometry optimizations have been performed for the X^3B_1, a^1A_1, b^1B_1 and c^1A_1 electronic states of CH_2, the X^2B_1 and A^2A_1 electronic states of NH_2 and the X^1A_1' electronic state of BH_3 using a DZP basis set. The results are compared with those obtained using the MRD-CI method at different levels of theoretical treatment. The agreement between the geometrical parameters optimized with the FCI and MRD-CI methods is very good.

Key words: Geometry optimization – FCI – MRD-CI

1 Introduction

The computation of stationary points on the potential energy hypersurface of different electronic states of molecular systems has been one of the main goals of quantum chemistry and many papers in the literature deal with this topic. The use of gradient techniques has made it feasible to find stationary points for polyatomic molecules using polyatomic wave functions with different levels of sophistication. At this point it would be convenient to have a benchmark of full configuration interaction (FCI) optimized geometries in order to compare different theoretical approaches.

In the past few years, a series of benchmark FCI calculations have been carried out on a set of model electronic systems at different nuclear geometries [1–15]. Such computations have been done using atomic orbitals (AO) basis sets up to double zeta plus polarization (DZP) quality and the results have been very useful to calibrate the accuracy of several electron correlation treatments. In this sense, Bauschlicher and coworkers [3–13] have provided a detailed comparison of FCI results with those of other methods. The benchmarks have shown that a multireference configuration interaction treatment gives a reasonable estimate of FCI energies, even at geometries far from equilibrium. Knowles et al. [16] have compared FCI results with multireference single and double excitation configuration interaction (MRD-CI) ones, while Illas et al. [17] compared FCI with CIPSI results. The only computations of stationary points at the FCI level, as far as we know, have been reported by Bauschlicher et al. [7] on the collinear transition state for

the reaction $F + H_2 \rightarrow HF + H$, where a grid of points spanning the region of the saddle point was computed and fitted to a polynomial, and the thermolecular reaction of $3H_2$ [14].

In the present work, we have carried out FCI geometry optimizations by using gradient techniques, for several electronic states (ground and excited), using a DZP basis set, with the aim that these results would serve as a calibration for other methods. Moreover, the FCI results are compared with MRD-CI [18–20] calculations performed at different levels of theoretical treatment.

The MRD-CI space is constructed considering all single and double excitations from a given set of reference electronic configurations. In constructing this space it is important to determine which set of reference configurations is necessary to describe a particular state in a wide range of nuclear arrangements. The relevance of some configurations may vary along the energy potential hypersurface and omission of an important reference configuration near a stationary point may lead to a wrong geometry prediction. At this point it is important to keep in mind that, as the number of reference configurations increases, the limit of the MRD-CI space generated is the FCI space. This feature is clearly shown in a particular example below. The number of generated configurations in a MRD-CI treatment grows rapidly as the number of electrons and/or the number of reference configurations increases. Thus it is important to test the results obtained with perturbatively corrected MRD-CI wave functions. In the standard MRD-CI method the configurations included in the CI space are chosen within a given selection threshold. Since geometry optimization using gradient techniques has to be done using a preset selected CI space, it may be critical to determine which selected CI space should be used. It is well known that the weight of many configurations in the CI wave function may change strongly with the molecular geometry. Thus the weight of the corresponding single and double excitations may also change. Consequently, given a suitable reference set of configurations, an incorrect selection of CI space may lead to wrong geometry predictions. Particular examples of this feature are discussed below.

In the next sections, we present a detailed comparison of the molecular geometries computed at the FCI and MRD-CI levels for the X^3B_1, a^1A_1, b^1B_1 and c^1A_1 states of CH_2, the X^2B_1 and A^2A_1 states of NH_2 and the X^1A_1' state of BH_3. First of all we compare the FCI results with those obtained at the MRD-CI level using a selection threshold of zero, hereafter denoted (MRD-CI, $T = 0$), analyzing in a particular example the effect of increasing the number of reference configurations. Secondly, we compare the (MRD-CI, $T = 0$) results with those obtained by choosing different values of the selection threshold, hereafter denoted (MRD-CI, $T > 0$) level in μhartree.

2 Computational methods and technical details

In the present study we have employed the Huzinaga–Dunning [21, 22] double-zeta basis set contracted as (9*s*5*p*/4*s*2*p*) for B, C and N, and (4*s*/2*s*) for H, with scaled exponents, augmented by polarization functions with orbital exponents $\alpha_d(B) = 0.7$ and $\alpha_d(N) = 0.85$, while for C we used $\alpha_d = 0.74$ and $\alpha_d = 0.51$ for states of B_1 and A_1, respectively, as suggested by Bauschlicher et al. [23]. For H we used $\alpha_p = 1.0$ as in Ref. [6]. In the FCI and MRD-CI calculations, only the valence electrons were explicitly correlated, namely, the 1*s* electrons of B, C and N were frozen as a core. In addition, for NH_2 and BH_3 the highest energy virtual orbital was excluded from the FCI and MRD-CI procedures.

The MRD-CI calculations were carried out by using the standard procedure of Buenker and Peyerimhoff [18–20] which employs the table CI algorithm [24]. Different levels of MRD-CI wave functions are considered in the present work. Since we are interested mainly in geometry optimization, we have omitted in the MRD-CI calculations the extrapolation procedure. A detailed comparison between MRD-CI extrapolated energies and FCI energies are given in Ref. [16]. In the (MRD-CI, $T=0$) calculations the effect of the unlinked clusters (simultaneous pair correlation) has been estimated by using the Davidson–Langhoff correction analogue for multireference wave functions [25–27] of Eq. (1).

$$\Delta E_{\mathrm{FCI}} = \left(1 - \sum_i (C_i)^2\right) \Delta E_{\mathrm{MRD\text{-}CI}}. \tag{1}$$

The sum runs over the squares of the coefficients C_i of the reference configurations and $\Delta E_{\mathrm{MRD\text{-}CI}}$ is the difference between the calculated MRD-CI energy and the obtained by solving the $M \times M$ reference secular equation, M being the number of symmetry adapted functions (SAFs) generated from the reference configurations. Hereafter such a correction will be denoted by (MRD-CI + Q). Throughout this work, the notation nM is used to describe the number of reference configurations.

The FCI calculations were performed by using a program [28] based on the σ vector procedure [29] for computing the effect of the electronic Hamiltonian matrix $\boldsymbol{H}$, on a trial vector $\boldsymbol{C}$ based on Slater determinants (SD). The technique of Handy [30] of separating the SD set into alpha strings and beta strings is used. Finally, following Olsen et al. [31], the electron contribution is divided into three terms, e.g. two-electron excitations in the alpha spin space, two-electron excitations in the beta spin space and two-electron excitations, one in the alpha and one in the beta spaces. The lowest-lying eigensolution of $\boldsymbol{H}$ is obtained using the three-term recurrence method proposed by van Lenthe and Pulay [32] improved by us [33]. This method also allows one to obtain roots of excited states if the trial vector $\boldsymbol{C}$ is quite close to the solution [33].

A new algorithm, recently reported by one of us [34], has been used in the geometry optimizations. This algorithm is based on the conjugated gradient technique, called Restricted Quasi-Newton–Raphson, as proposed by Fletcher [35]. The molecular geometries are considered optimized when the gradient norm is lower than 10^{-5}. Gradients were calculated numerically. Since the CI energy is stationary with respect to first-order variations of the CI parameters, the energy derivative is evaluated in the following way:

$$\frac{\partial E}{\partial x_i} = \sum_{ijkl} \frac{\partial \{ij|kl\}}{\partial x_i} \Pi_{ijkl}, \tag{2}$$

where Π_{ijkl} is an element of the two-electron reduced density matrix, $\{ij|kl\}$ is an element of the two-electron average Hamiltonian or Bopp matrix [36] and x_i a nuclear coordinate. The i, j, k, l, indixes denote molecular orbitals (MOs). The Bopp matrix is defined as

$$\{ij|kl\} = \left\{\frac{1}{2}\left[\frac{1}{N}\left(\left(h_{ij} - \frac{1}{2}\sum_m (im|mj)\right)\delta_{kl} + \delta_{ij}\left(h_{kl} - \frac{1}{2}\sum_m (km|ml)\right)\right) + (ij|kl)\right]\right\}, \tag{3}$$

where h_{ij} are the one-electron integrals, $(ij|kl)$ are the two electron integrals and N is the total number of the electrons in the molecule. The latter definition implies that the Π matrix is evaluated as

$$\Pi_{ijkl} = \langle \Psi | \hat{E}_{ij}\hat{E}_{kl} | \Psi \rangle, \tag{4}$$

where $\hat{E}_{ij}$ are the so-called shift operators [37] and Ψ is the electronic state wave function. The derivative of the Bopp operator is computed by finite differences, namely, the self-consistent field (SCF) MOs are computed at the perturbed molecular geometry, then the Bopp matrix (3) is constructed and, finally, the energy derivative is calculated by using Eq. (2).

3 Results and discussion

As indicated above, the results presented in this section will be analyzed from two different points of view. Firstly, we compare the results obtained at the FCI and (MRD-CI, $T=0$) levels of theory. The main goal is to investigate the behavior of both treatments from the geometry-optimization point of view. Secondly, we will analyze the behavior of the perturbatively selected CI space (MRD-CI, $T>0$) along the geometry-optimization process.

3.1 Low-lying electronic states of CH_2

The X^3B_1, a^1A_1 and c^1A_1 electronic states of methylene have received a great deal of attention, both from an experimental and theoretical point of view [38–47], and have been used to perform benchmark FCI single-point calculations [6, 9]. We have optimized the equilibrium geometry of these states and also those corresponding to the b^1B_1 electronic state. The adiabatic excitation energies calculated at the FCI and (MRD-CI, $T=0$) levels are given in Table 1.

3.1.1 X^3B_1 and b^1B_1 states

The geometrical results obtained for the X^3B_1 and b^1B_1 states of CH_2 are displayed in Table 2. Both states are well described by a single electronic configuration, namely, $1a_1^2 2a_1^2 1b_2^2 3a_1 1b_1$. For both states we have used the SCF MOs of the X^3B_1 state to carry out the CI calculations. The SCF treatment gives a correct description of the X^3B_1 state with an error in the HCH angle of about 3.5° as compared with the experimental value [47].

The agreement between (FCI) and (MRD-CI, $T=0$) results is very good, and the error in α(HCH) is of 0.1° for both triplet and singlet states, respectively. The latter is particularly relevant if one takes into account the dimensions of the eigenvalue problems solved, namely, 943 724 SDs (FCI) versus 9039 SAFs (MRD-CI, $T=0$) for the triplet and 1 311 624 SDs (FCI) versus 8098 SAFs (MRD-CI, $T=0$) for the singlet. The adiabatic excitation energy calculated at the (MRD-CI, $T=0$) and FCI levels for the b^1B_1 state are in excellent agreement.

As mentioned in Sect. 1, the accuracy of the results obtained at truncated MRD-CI levels, namely, (MRD-CI, $T>0$), depends on both the molecular geometry at which the CI space is selected and the selection threshold. Thus, for X^3B_1, starting at R(CH) = 1.05 Å and α(HCH) = 110.0° the optimized value of the

Table 1. Calculated adiabatic excitation energies (in eV) at different levels of theoretical treatment[a]

State	FCI	MRD-CI	MRD-CI +Q
CH_2			
X^3B_1	0.00	0.00	0.00
a^1A_1	0.52[b]	0.54[b]	0.51[b]
	0.52[c]	0.56[c]	0.51[c]
b^1B_1	1.67	1.66	1.66
c^1A_1	2.83	2.82	2.82
NH_2			
X^2B_1	0.00	0.00	0.00
A^2A_1	1.47	1.46	1.48

[a] Results obtained combining the energies given in the footnotes of Tables 2–5

[b] CI calculations carried out with the MO basis of $^3B_1$

[c] CI calculations carried out with the MO basis of $^1A_1$

Table 2. Comparison of the equilibrium geometries calculated at different levels of theory for the X^3B_1 and b^1B_1 states of CH_2[a]

Method	Dimension[b]	Initial geometry		Final geometry[c]			
		R(CH)	α(HCH)	R(CH)	α(HCH)	ΔR[d]	$\Delta\alpha$[d]
X^3B_1							
SCF	1	1.05	110.0	1.074	129.4		
MRD-CI (4M):							
$T=3$	1351	1.05	110.0	1.083	130.8	−0.001	−1.6
$T=1$	1610	1.05	110.0	1.083	131.6	−0.001	−0.8
$T=3$	1336	1.074	129.4	1.083	132.3	−0.001	−0.1
$T=1$	1604	1.074	129.4	1.083	132.1	0.0	−0.3
$T=0$	9039	1.05	110.0	1.084	132.4	0.0	−0.1
FCI	943 724	1.05	110.0	1.084	132.5		
b^1B_1							
MRD-CI (8M):							
$T=3$	1032	1.074	129.4	1.080	140.1	0.0	−1.2
$T=1$	1387	1.074	129.4	1.081	140.3	0.0	−1.0
$T=0$	8098	1.074	129.4	1.081	141.3	0.0	0.1
FCI	1 311 624	1.074	129.4	1.081	141.2		

[a] Bond distances in Å and bond angles in degrees

[b] Number of SDs (FCI) or SAFs (MRD-CI) of the CI space

[c] The energies (in hartree) at the optimum geometries are:
– for X^3B_1: −38.928217 (SCF), −39.043809 (MRD-CI, $T=0$), −39.047989 (MRD-CI +Q) and −39.046266 (FCI)
– for b^1B_1: −39.982766 (MRD-CI, $T=0$), −38.987020 (MRD-CI +Q) and −39.984927 (FCI)

[d] For the (MRD-CI, $T>0$) results ΔR and $\Delta\alpha$ are defined as the difference between the values of these parameters optimized at the (MRD-CI, $T>0$) and (MRD-CI, $T=0$) levels, while for the (MRD-CI, $T=0$) results as the difference between the values optimized at the (MRD-CI, $T=0$) and FCI levels

latter parameter differs by $-1.6°$ (MRD-CI, $T=3$) and $-0.8°$ (MRD-CI, $T=1$) from the value optimized at the (MRD-CI, $T=0$) level. Starting at the SCF optimized geometry, namely, $R(CH)=1.074$ Å and $\alpha(HCH)=129.4°$, these differences are reduced to $-0.1°$ (MRD-CI, $T=3$) and $-0.3°$ (MRD-CI, $T=1$). For b^1B_1, similar trends are observed regarding the selection threshold, with differences of 1.0° in α(HCH) and 0.0 Å in R(CH) for (MRD-CI, $T=1$). From Table 2 we conclude that good results are obtained for the X^3B_1 and b^1B_1 states solving secular problems of 1604 and 1387 SAFs respectively. On the other hand, the amount of computation time saved with respect to the (MRD-CI, $T=0$) calculations, which involve a secular problem of about 9000 SAFs, is substantial.

3.1.2 *The a^1A_1 state*

The a^1A_1 state has two important configurations at the equilibrium geometry (the FCI coefficients are $-0.95\ [1a_1^2 2a_1^2 3a_1^2 1b_2^2] + 0.18[1a_1^2 2a_1^2 1b_1^2 1b_2^2]$). Benchmark FCI calculations on the energy splitting between X^3B_1 and a^1A_1 have been extensively analyzed by Bauschlicher et al. [6] using the same DZP basis set and compared with MRCI calculations. Knowles et al. [16] compared resulted of FCI and MRD-CI calculations carried out at different selection thresholds. In the present work we compare the optimized geometries computed at the FCI and MRD-CI levels. We are also interested in analysing the dependence of the results on the orbital basis. Therefore, we have repeated for each theoretical treatment the geometry optimization with the SCF vectors of the X^3B_1 and a^1A_1 states. Results are summarized in Table 3.

The geometries optimized at the FCI level using both orbital basis sets are identical ($R(CH)=1.120$ Å and $\alpha(HCH)=101.8°$). The energy differs by 3.5×10^{-5} hartree. Similar FCI energy dependence on the orbital basis has been described by Bauschlicher et al. [4] in benchmark FCI calculations on HF and NH_2. These authors indicate that the slight difference arises from the frozen-core approximation constraint. Probably, the fact of keeping fixed the exponents of the AO basis also has a minor effect.

Calculations carried out at the (MRD-CI, $T=0$) level provide results of very good quality in both orbital basis. For the geometrical parameters R(CH) and α(HCH), the differences are less than 0.003 Å and 0.4°, respectively. The calculated excitation energy (see Table 1) differs from the FCI result by 0.02–0.04 eV at (MRD-CI, $T=0$) and 0.01 eV at (MRD-CI + Q), depending on the orbital basis used.

Further calculations carried out at truncated MRD-CI levels show the same trends observed for the X^3B_1 state. Similar results are obtained using both orbital basis. Again, the reduction of the computational effort is evident as shown by the dimensions of the secular problems in each case (Table 3).

3.1.3 *The c^1A_1 state*

A previous theoretical study by Römelt et al. [41] on the c^1A_1 state indicates that it prefers a linear equilibrium geometry. In a linear geometry this state becomes a $^1\Sigma_g^+$ state possessing the $(\pi_y^2+\pi_x^2)$ electronic configuration, which in the lower symmetry subgroup C_{2v} corresponds to the $(1b_1^2+3a_1^2)$ configuration (see Table 3 of Ref. [43]). Consequently, the $1a_1^2 2a_1^2 3a_1^2 1b_2^2$ and $1a_1^2 2a_1^2 1b_1^2 1b_2^2$ configurations

Table 3. Comparison of the equilibrium geometries calculated at different levels of theory for the a^1A_1 state of CH_2[a]

Method	Dimension[b]	Initial geometry		Final geometry[c]			
		R(CH)	α(HCH)	R(CH)	α(HCH)	ΔR[d]	$\Delta\alpha$[d]
A) SCF vectors of X^3B_1							
MRD-CI (8M):							
$T=3$	919	1.05	110.0	1.114	103.8	−0.004	1.6
$T=1$	1277	1.05	110.0	1.115	102.7	−0.002	0.6
$T=0$	6139	1.05	110.0	1.117	102.1	0.002	0.3
FCI	1 333 768	1.05	110.0	1.120	101.8		
B) SCF vectors of a^1A_1							
MRD-CI (7M):							
$T=3$	898	1.05	110.0	1.114	103.6	−0.003	1.5
$T=1$	1235	1.05	110.0	1.115	102.8	−0.002	0.6
$T=0$	6871	1.05	110.0	1.117	102.2	−0.003	0.4
FCI	1 333 768	1.05	110.0	1.120	101.8		

[a] Bond distances in Å and bond angles in degrees

[b] Number of SDs (FCI) or SAFs (MRD-CI) of the CI space

[c] The energies (in hartree) at the optimized geometries are:

1) Using SCF vectors of $^3B_1$: −39.023806 (MRD-CI, $T=0$), −39.029406 (MRD-CI +Q) and −39.027163 (FCI)

2) Using SCF vectors of $^1A_1$: −39.023379 (MRD-CI, $T=0$), −39.029331 (MRD-CI +Q) and −39.027198 (FCI)

[d] See footnote d of Table 2

in C_{2v} symmetry, hereafter refered to configurations A and B, respectively, should have the same coefficient in the wave function at the linear geometry. Moreover, in bent geometries, both configurations should be included in any CI treatment.

We began the geometry optimization at α (HCH) = 110° using the SCF vectors of the X^3B_1 state in all CI calculations. The results are shown in Table 4. Unexpectedly, the FCI calculations led to a bent optimized geometry (α(HCH) = 168.5°), the coefficients of the A and B configurations in the wave function being 0.63 and 0.73, respectively.

Different types of MRD-CI treatments were employed. First of all, at the (MRD-CI, $T=0$) level we optimized the geometry using different sets of reference configurations denoted as nM. As nM increases, higher excitations are included in the MRD-CI wave function and, therefore, the CI approaches to the FCI limit. Here, by a FCI limit we mean both the molecular geometry and energy calculated at the FCI level. The results are displayed in Table 4, while Fig. 1 shows the errors obtained in each (MRD-CI, $T=0$) treatment with respect to the FCI limit as nM increases. For the sake of simplicity, we show only the errors in α(HCH) and the energy calculated at the (MRD-CI, $T=0$) and (MRD-CI +Q) levels, but not the errors in the CH distance.

When only the two configurations A and B are considered as the reference set (2*M*), there are only single and double excitations in the MRD-CI space. The geometry optimization leads to a linear geometry. The error in the CH distance is 0.005 Å and the diagonalized energy differs by 7.0×10^{-3} hartree from the FCI energy. In the (MRD-CI, $T=0$) 2M wave function the two configurations A and B have the same weight (C_i^2 percentage is 46.85%), as expected for a linear geometry.

Table 4. Comparison of the equilibrium geometries calculated at different levels of theory for the c^1A_1 state of CH_2[a]

Method	Dimension[b]	Final geometry R(CH)	α(HCH)	Energy[c]	$\Sigma_i C_i^2$	
MRD-CI, $T=0$						
2*M*	1232	1.070	180.0	−38.935291	(−38.943667)	0.937
4*M*	1964	1.079	170.3	−38.936920	(−38.943945)	0.943
10*M*	5218	1.074	169.1	−38.939340	(−38.944239)	0.955
15*M*	9975	1.075	168.1	−38.940054	(−38.944208)	0.959
19*M*	13 271	1.075	168.5	−38.940838	(−38.943862)	0.965
26*M*	18 875	1.075	168.5	−38.941403	(−38.943593)	0.971
33*M*	23 028	1.075	168.7	−38.941697	(−38.943344)	0.975
FCI	1 333 768	1.075	168.5	−38.942333		

[a] Bond distances in Å and bond angles in degrees
[b] Number of SDs (FCI) or SAFs (MRD-CI) of the CI space
[c] MRD-CI +Q energies are given in parentheses

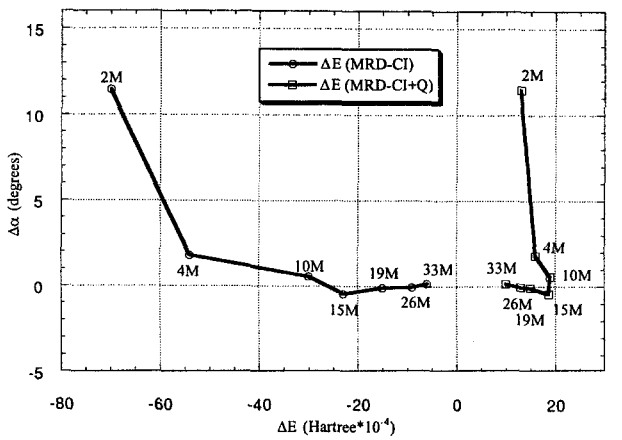

Fig. 1. Errors of MRD-CI, $T=0$ with respect to FCI limit as M increases. The FCI limit corresponds to the origin of coordinates

The next two sets of reference configurations (4*M* and 10*M*) generate up to quadruple excited configurations in the MRD-CI space. With this treatment the error in the geometrical parameters is reduced significantly. All the remaining sets of reference configurations (15*M*, 19*M*, 26*M* and 33*M*) generate up to sextuple excitations and from Fig. 1 it is clearly seen that the results converge to the FCI limit. The best calculations (33*M*) are in an excellent agreement with the FCI results. This is particularly important if one takes into account the dimensions of the different secular problems involved, namely 1 333 768 SD in the FCI case versus only 23 028 SAF in the best MRD-CI calculations. Note that small MRD-CI spaces conveniently generated provide results as good as the FCI ones. (See Table 4).

Another point of interest is to observe the behaviour of the Davidson correction (MRD-CI +Q) shown schematically in the right-hand side of Fig. 1. The (MRD-CI +Q) calculated energies are in all cases below the FCI energy, as indicated by the positive sign of the error. When the quality of the wave functions is increased by augmenting the number of reference configuration, the error first augments (up to

1.0×10^{-3} hartree for the $10M$ set) but decreases progressively (to 1.0×10^{-3} hartree for the $33M$ set) converging to the FCI limit. However, in all cases, the error in the Davidson correction is in the range 1.0×10^{-3}–1.9×10^{-4} hartree.

The excitation energy calculated at the (MRD-CI, $T = 0$) level is in very good agreement with the FCI result, as shown in Table 1. For the c^1A_1 state we took the energy values of the $15M$ set, because it provides an MRD-CI wave function of the same quality as that obtained for the X^3B_1 state.

Since we were surprised to find a bent equilibrium geometry for c^1A_1 we decided to go a step further and calculate the inversion barrier. The calculations were done at the FCI, (MRD-CI, $T = 0$) $15M$ and (MRD-CI, $T = 0$) $33M$ levels. Obviously, in all cases the inversion occurs at $\alpha(\mathrm{HCH}) = 180°$. We checked that in this stationary point the approximate hessian possesses a single negative eigenvalue. For this transition state, the optimized CH distances in Å at differet levels of theory are (R(CH) in Å) 1.073 (FCI), 1.073 (MRD-CI, $15M$) and 1.073 (MRD-CI, $33M$) and the energies (in hartree) are: −38.942114 (FCI), −38.939878 (−38.943910) (MRD-CI, $15M$) and −38.941520 (−38.942925) (MRD-CI, $33M$) (MRD-CI +Q values in parenthesis).

According to these results, we find that the inversion barrier is less than 49 cm^{-1} in the FCI case. Therefore, we are sceptical regarding the result that c^1A_1 has a bent equilibrium geometry. This unexpected result may be addressed to two different facts. First the effect of having frozen the $1s$ electron as a core, since in this case FCI results are not exactly invariant because the frozen core and second the poor quality of the basis set. Correlating all electrons leads to a FCI problem greater than 40×10^6 SDs that is outside of our computer capabilities, but we have carried out a further (MRD-CI, $T = 0$) optimization with eight electrons. We have included 18 configurations in the reference set, which leads to a secular problem of 29 812 SAFs and a wave function whose $\Sigma_i C_i^2$ is 0.964. The optimized parameters are $R(\mathrm{CH}) = 1.074$ Å and $\alpha(\mathrm{HCH}) = 168.1°$. Computations of such quality have been proved to give results that agree very well with the FCI ones and therefore we are confident that FCI calculations would provide similar results. We believe that this may be an effect of the poor quality of the basis set used. We think further investigations should be done in this sense. However, the results obtained in this work indicate that the potential energy surface of this state is very flat. On the other hand, one may conclude that the MRD-CI method reproduces the FCI calculated molecular geometries and energies very well.

3.2 The X^2B_1 and A^2A_1 states of NH_2

Several theoretical studies exist in the literature for the X^2B_1 and A^2A_1 states of NH_2 [48–51] and Benchmark FCI calculations with a DZP basis have been carried out at different geometries [4]. These FCI results have been compared with those obtained from different correlation methods (SDCI, SDTQCI, CPF, MRCI) [4], including MRD-CI at different levels of truncation [16]. For these states we have carried out the same treatments given above for CH_2. The results are displayed in Table 5. Since we are interested in analyzing the effect of optimizing a particular state at the MRD-CI level, using an orbital basis from the another state, all CI calculations were done in the basis of the SCF orbitals of the X^2B_1 state.

Table 5. Comparison of the equilibrium geometries calculated at different levels of theory for the X^2B_1 and A^2A_1 states of NH_2[a]

Method	Dimension[b]	Initial geometry		Final geometry[c]			
		R(NH)	α(HNH)	R(NH)	α(HNH)	ΔR[c]	$\Delta\alpha$[c]
X^2B_1							
SCF	1	1.10	120.0	1.012	105.0		
MRD-CI (4M):							
$T=3$	1445	1.10	120.0	1.028	104.6	−0.002	1.3
$T=1$	1715	1.10	120.0	1.028	104.0	−0.001	0.7
Ref CI[d]	9	1.10	120.0	1.017	106.2		
$T=3$	1428	1.00	106.0	1.027	103.6	−0.002	0.4
$T=1$	1661	1.00	106.0	1.028	103.5	−0.002	0.2
$T=0$	11530	1.10	120.0	1.029	103.2		
FCI	5373494	1.10	120.0	1.032	102.9		
A^2A_1							
MRD-CI (5M):							
$T=3$	1371	1.10	120.0	1.0	142.1	0.0	−1.3
$T=1$	1822	1.10	120.0	1.0	142.3	0.0	−1.1
Ref CI[d]	11	1.10	120.0	0.991	149.0		
$T=3$	1377	1.00	149.0	0.998	144.1	−0.002	0.7
$T=1$	1751	1.00	149.0	1.0	143.9	−0.001	0.4
$T=0$	11113	1.10	120.0	1.0	143.5	−0.002	0.2
FCI	5381446	1.10	120.0	1.001	143.3		

[a] Bond distances in Å and bond angles in degrees

[b] Number of SDs (FCI) or SAFs (MRD-CI) of the CI space

[c] Energies (in hartree) at the optimized geometries are:

1) for X^2B_1: −55.573522 (SCF), −55.737785 (MRD-CI, $T=0$), −55.745157 (MRD-CI +Q) and −55.743324 (FCI)

2) for A^2A_1: −55.684167 (MRD-CI, $T=0$), −55.690797 (MRD-CI +Q) and −55.689196 (FCI). Calculations over X^2B_1 vectors

[d] See footnote d of Table 2

The (MRD-CI, $T=0$) and FCI results are in an excellent agreement. The errors in the geometrical parameters are 0.003 Å (NH distance) and 0.3° (α(HNH)) for X^2B_1 and 0.002 Å (NH distance) and 0.2° (α(HNH)) for A^2A_1. Moreover, the excitation energies (see Table 1) calculated at the (MRD-CI, $T=0$) and (MRD-CI +Q) levels, are also in very good agreement, the errors being only 0.01 eV with respect to FCI. The effect of the orbital basis appears to be unimportant in optimizing equilibrium geometries at the MRD-CI level. It is also worth emphasizing again that (MRD-CI, $T=0$) provides results of FCI quality while solving secular problems of modest size. Thus Table 5 shows that the FCI space has about 5400000 SDs, while the MRD-CI space contains only about 12000 SAFs.

Further reduction of the computational effort can also be achieved by using selected MRD-CI spaces, the dimensions of the secular problems being reduced to 1371–1822 SAFs (see Table 5). Beginning at α(HNH) = 120°, far from the equilibrium geometry of both states, we obtain optimized geometries with errors between 0.7–1.3° in the α(HNH) angle. A better choice of the starting points could be the SCF-optimized geometry, because both states are well described at this level of theory. However, in many cases, there is not an adequate single-configuration description of a given electronic state, so a different starting point should be taken.

Table 6. Comparison of equilibrium geometries calculated at different levels of theory for the X^1A_1' state of BH_3[a]

Method	Dimension[b]	Initial geometry R(BH)	Final geometry[c] R(BH)	ΔR[d]
SCF	1	1.10	1.192	
SDCI	1002	1.19	1.191	− 0.002
MRD-CI (5M):				
$T=3$	771	1.19	1.192	− 0.001
$T=1$	961	1.19	1.192	− 0.001
$T=0$	7964	1.19	1.192	− 0.001
FCI	3 368 924	1.19	1.193	

[a] Bond distances in Å and bond angles in degrees
[b] Number of SDs (FCI) or SAFs (MRD-CI) of the CI space
[c] Energies (in hartree) at the optimized geometry are: − 26.392443 (SCF), − 26.499524 (SD-CI), − 26.504416 (SD-CI + Q), − 26.501573 (MRD-CI, $T=0$), − 26.505119 (MRD-CI + Q) and − 26.504049 (FCI)
[d] See footnote d of Table 2

Since in any multireference CI treatment good results are achieved when the set of reference configurations accounts for about 90% of the wave function, it is likely that such a reference set gives a good zero-order description of a particular state. Therefore, to get good starting points we optimized the geometries of both states using a $M \times M$ CI space, where M is the number of SAFs generated by the reference configurations. These CI spaces are denoted as Ref CI in Table 5. The optimized geometries at this CI level were taken as starting points for the subsequent truncated MRD-CI calculations. In this way, we obtained very good results at the truncated MRD-CI level, depending on the selection threshold (see Table 5), with little computational effort.

3.3 The X^1A_1' ground state of Borane

The last example we have studied is the ground state of BH_3. For this system, the calculations were performed at the SCF, SDCI, MRD-CI and FCI levels of theory. The dimensions of the secular problems solved in the different CI approaches ranges from 771 to 7961 SAFs, while the FCI calculations involved a CI space of 3 368 924 SDs. All calculations were done in the C_{2v} symmetry group. Table 6 collects the results.

The ground state of Borane is well described by a single configuration (the leading determinant in the FCI wave function has a coefficient of 0.9738). Consequently, it is likely that all theoretical methods provide good results. In fact, the errors in the calculated BH distance with respect to the FCI value are less than 0.002 Å. The truncated MRD-CI calculations involving small secular problems provide very good results, even better than those of the SDCI approach. The optimized equilibrium geometry is similar to both the experimental and theoretical report in the literature [52–55]. The errors in the calculated energy (hartree) with respect to the FCI value show the same trends pointed out above, namely

−0.004525 (SDCI), 0.000367 (SDCI + Q), −0.002476 (MRD-CI, $T=0$) and 0.00170 (MRD-CI +Q) μhartree. It is worth noting that the (SDCI +Q) energy approaches more to the FCI value than the (MRD-CI +Q) energy. However, augmenting the number of reference configurations the errors in the MRD-CI and MRD-CI +Q energies should decrease, as shown explicitly in Fig. 1 for the c^1A_1 state of CH_2.

4 Summary and conclusions

We have reported the equilibrium geometries for various electronic states of CH_2, NH_2 and BH_3 optimized using FCI and MRD-CI methods with a DZP basis set. In all cases, the results obtained at the (MRD-CI, $T=0$) and FCI levels of theory are in an excellent agreement. For the a^1A_1 state of CH_2, the geometry optimization has been carried out in all CI treatments using two different orbital basis sets, namely, the SCF vectors of the X^3B_1 and a^1A_1 states. The equilibrium geometries obtained in both cases are nearly identical. The c^1A_1 state of CH_2 is predicted to have a bent equilibrium geometry with a barrier to linearity lower than 50 cm^{-1} at the FCI level. Consequently, further investigations with better basis sets should be undertaken to ascertain the true equilibrium geometry of this state. The MRD-CI method appears to reproduce the FCI potential energy surface very well. Finally, the geometrical parameters optimized with a truncated MRD-CI treatment compare very well with those obtained at the (MRD-CI, $T=0$) level, despite the substantial reduction of the computational effort involved.

Acknowledgements. This research was supported by the Spanish DGI-CYT (Grants PB92-076-C02-01 and PB92-0796-C02-02). We are also grateful to Professors R.J. Buenker and S.D. Peyerimhoff for providing us the MRD-CI program package and to Professors S. Olivella and A. Solé for encouragement and valuable discussions. The calculations were carried out on IBM/RS 6000 models 375 and 58H workstations.

References

1. Saxe P, Schaefer HF III (1981) Chem Phys Lett 79:202
2. Harrison RJ, Handy NC (1983) Chem Phys Lett 95:386
3. Bauschlicher CW Jr, Taylor PR (1986) J Chem Phys 85:2779
4. Bauschlicher CW Jr, Langhoff SR, Taylor PR, Knowles PJ (1986) J Chem Phys 85:1469
5. Bauschlicher CW Jr, Langhoff SR, Partridge H, Taylor PR (1986) J Chem Phys 85:3407
6. Bauschlicher CW Jr, Taylor PR (1986) J Chem Phys 85:6510
7. Bauschlicher CW Jr, Taylor PR (1987) J Chem Phys 86:858
8. Bauschlicher CW Jr (1987) J Chem Phys 86:5591
9. Bauschlicher CW Jr, Taylor PR (1987) J Chem Phys 86:2844
10. Bauschlicher CW Jr, Langhoff SR (1987) J Chem Phys 86:5595
11. Bauschlicher CW Jr, Taylor PR (1987) J Chem Phys 86:5600
12. Bauschlicher CW Jr, Langhoff SR (1988) J Chem Phys 89:2116
13. Bauschlicher CW Jr, Langhoff SR (1988) J Chem Phys 89:4246
14. Taylor PR, Komornicki A, Dixon DA (1989) J Am Soc Chem Phys 111:1259
15. Bauschlicher CW Jr, Langhoff SR, Taylor PR (1990) Adv Chem Phys 77:103
16. Knowles DB, Alvarez-Collado JR, Hirsch G, Buenker RJ (1990) J Chem Phys 92:585; Buenker RJ, Knowles DB, Rai SN, Hirsch G, Bhanuprakash K, Alvarez-Collado JR (1989) In: Carbo R (ed), Studies in physical and theoretical chemistry, vol. 62, Quantum Chemistry-Basic Aspects, Actual Trends, Elsevier, Amsterdam p. 181

17. Illas F, Rubio J, Ricart JM, Bagus PS (1991) J Chem Phys 95:1877
18. Buenker RJ, Peyerimhoff SD (1974) Theor Chim Acta 35:33
19. Buenker RJ, Peyerimhoff SD (1975) Theor Chim Acta 39:217
20. Buenker RJ, Peyerimhoff SD, Butscher W (1978) Mol Phys 35:771
21. Huzinaga S (1965) J Chem Phys 42:1293
22. Dunning TH Jr (1970) J Chem Phys 53:2823
23. Bauschlicher CW Jr, Shavitt I (1978) J Am Chem Soc 100:739
24. Buenker RJ (1980) In: Burton P (ed), Proc workshop on quantum chemistry and molecular physics in Wollongong, Australia, University Press, Wollongong; Buenker RJ (1982) in: Carbó R (ed), Studies in physical and theoretical chemistry, vol. 21, Current Aspects of Quantum Chemistry, Elsevier, Amsterdam, p. 17: Buenker RJ, Phillips RA (1985) J Mol Struct Theochem 123:291
25. Langhoff SR, Davidson ER (1973) Int J Quantum Chem 7:999; Davidson ER (1974) In: Daudel R, Pullman B (ed), The World of quantum chemistry, Reidel, Dordretch, p. 17
26. Bruna PJ, Peyerimhoff SD, Buenker RJ (1980) Chem Phys Lett 72:278
27. Hirsch G, Bruna PJ, Peyerimhoff SD, Buenker RJ (1977) Chem Phys Lett 52:442
28. FCI program written by Anglada JM, Bofill JM copyright of CID-CSIC and Universitat de Barcelona
29. Roos BO (1972) Chem Phys Lett 15:153
30. Handy NC (1980) Chem Phys Lett 74:280
31. Olsen J, Roos BO, Jørgensen P, Jensen JA (1988) J Chem Phys 89:2185
32. van Lenthe JH, Pulay P (1990) J Comput Chem 11:1164
33. Bofill JM, Anglada JM (1994) Chem Phys 183:19
34. Bofill JM (1994) J Comput Chem 15:1
35. Fletcher R (1987) Practical methods of optimization, Wiley, New York
36. Bopp F (1959) Z Phys 156:348
37. Duch W, Karwowski J (1985) Comput Phys Rep 2:93
38. Wadt WR, Goddard WA III (1974) J Am Chem Soc 96:5996
39. Luchesse RR, Schaefer HF III (1977) J Am Chem Soc 99:6765
40. Roos BO, Siegbahn PM (1977) J Am Chem Soc 99:7716
41. Römelt J, Peyerimhoff SD, Buenker RJ (1981) Chem Phys 54:147
42. Bunker PR, Sears TJ (1985) J Chem Phys 83:4866
43. Shavitt I (1985) Tetrahedron 41:1531
44. Goddard WA III (1985) Science 227:917
45. Schaefer HF III (1986) Science 231:1100
46. Carter EA, Goddard WA III (1987) J Chem Phys 86:862
47. Jensen P, Bunker PR (1988) J Chem Phys 89:1327
48. Bender CF, Schaefer HF III (1971) J Chem Phys 55:4798
49. Bell S, Schaefer HF III (1977) J Chem Phys 67:5173
50. Peyerimhoff SD, Buenker RJ (1979) Can J Chem 57:3182
51. Buenker RJ, Peric M, Peyerimhoff SD, Marian R (1981) Mol Phys 43:987
52. Curtiss LA, Pople JA (1988) J Chem Phys 89:614
53. Botschwina P (1989) In: Maier JP (ed), Ion and cluster ion spectroscopy, Elsevier, Amsterdam
54. Kawaguchi K (1992) J Chem Phys 96:3411
55. Martin JML, Lee TJ (1992) Chem Phys Lett 200:502